Asian Journal of Chemistry; Vol. 26, No. 18 (2014), 6292-6294

ASIAN JOURNAL OF CHEMISTRY

http://dx.doi.org/10.14233/ajchem.2014.18488

Synthesis and Optical Properties of ZnO Nanoneedles Array†

B. TANG*, Q. ZHANG, Q. LUO, Z.H. WU and Y. QIU

School of Science, Southwest Petroleum University, Chengdu, P.R. China

*Corresponding author: Tel: +86 13688038695; E-mail: atangbin@126.com

Received: 21 July 2014; *Accepted*: 22 August 2014; *Published online*: 1 September 2014; AJC-15902

Zinc oxide nanoneedles array were synthesized on Si substrate by catalyst-free chemical vapor deposition technique. Scanning electron microscopic images displayed that the ZnO nanoneedles with average diameter of 100 nm were aligned well on Si substrate. TEM images showed that there were some steps on the top of ZnO nanoneedles. Only (002) diffraction peak of ZnO can be found in the XRD patterns of the samples, indicating that the as-grown nanoneedles are highly crystalline in nature and grow along the [0001] direction. The growth mechanism of ZnO nanoneedles array is consistent with step kinetics and bizarre surface growing and the crystal growth is a typical simple-two-dimensional-nucleation normal-layer-growth. Room-temperature photoluminescence spectrum of ZnO nanoneedles array showed two near band-edge emission peaks at 380 and 389 nm and a deep level emission around 480 nm.

Keywords: ZnO nanoneedles array, Step kinetics, Bizarre surface, Photoluminescence.

INTRODUCTION

Zinc oxide (ZnO), a semiconductor with wide direct band gap (3.37 eV) and large exciton binding energy (60 meV), has received much attention attributed to various potential applications in the opto-electronic field, such as piezoelectric transducers, varistors, phosphors and surface acoustic wave (SAW) devices[1-4]. In recent years, one-dimensional (1-D) vertically aligned ZnO nanostructures have been fabricated for field emission display (FED) because of their high efficiency, low cost and small device size compared to conventional thermionic emitters[5,6]. Different fabrication methods including anodic aluminum oxide (AAO) template method[7], vapour transfer process[8], metal organic chemical vapour deposition (MOCVD)[9,10], hydrothermal synthesis[11] and thermal evaporation[12] have been widely reported for the preparation of one-dimensional ZnO nanostructures on Si or sapphire substrate[9,13].

In this work, ZnO nanoneedles array was synthesized on Si(111) substrate by thermal evaporation of ZnO powder without catalyst. The growth mechanism of ZnO nanoneedles array is consistent with step kinetics and bizarre surface growing and the crystal growth is a typical simple-two-dimensional-nucleation normal-layer-growth. The optical properties of the ZnO nanoneedles array were characterized by using photoluminescence spectrum.

EXPERIMENTAL

N-Type silicon (111) of 10 mm × 10 mm in size was used as the substrate. The substrate was first etched by 5 % HF solution for 2 min to remove any oxide on the surface, cleaned ultrasonically with acetone and ethanol in sequence and then dried at room temperature. As shown in Fig. 1, an alumina boat containing ZnO (99.99 %) powder was loaded in the center of horizontal alumina tube with the diameter of 20 cm. Meanwhile, the Si substrate facing up was loaded in the alumina tube 25 cm away from the alumina boat. The alumina chamber was evacuated to a pressure of 200-300 Torr and heated to 1350 ºC for 25 min. High-purity Ar (99.99 %) gas passed through the chamber with the gas flow rate of 40.0 sccm. Then the alumina chamber was heated to 1450 ºC for 5 min. The temperature difference between the source material and substrate was 700 ºC.

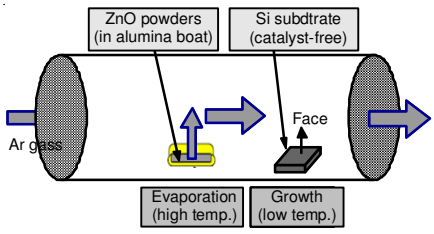

Fig. 1. Apparatus for the synthesis of ZnO nanoneedles array

†Presented at The 3rd Global Conference on Materials Science and Engineering (CMSE2014) held on 20-23 Oct. 2014, Shanghai, P.R. China

Characterization of ZnO nanoneedles was carried out with scanning electron microscopy (SEM) (JEOL-EDAX, Japan), high resolution transmission electron microscopy (HRTEM) (Tecnai G2 F20 S-TWIN, USA), X-ray diffraction (XRD) (Bede D1 System X, UK) and fluorescence spectrophotometer (RF-5301PC, Japan).

RESULTS AND DISCUSSION

The phase of the as-grown ZnO nanoneedles and their crystallographic orientation were identified by the XRD spectrum as shown in Fig. 2. Being indexed based on the hexagonal structure of bulk ZnO (JCPDS No. 80-0074), the XRD pattern indicates that the nanoneedles are highly oriented in [0001] direction and their crystallographic phase belongs to the wurtzite structure. The calculated lattice parameter of ZnO nanoneedles is 0.52 nm. No other peaks of aurum or impurity phases are found in any of our ZnO nanoneedles samples.

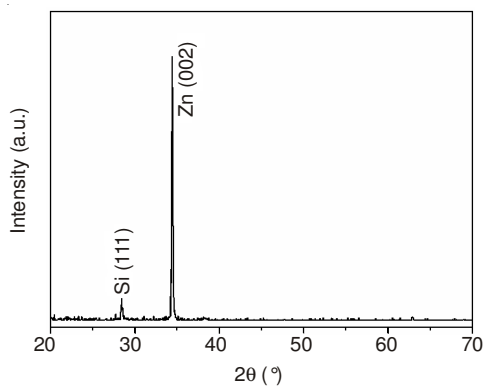

Fig. 2. XRD pattern of ZnO nanoneedles array

To obtain more details about the microstructure and composition of the prepared samples, SEM and HRTEM characterization were carried out. As shown in Fig. 3A,B, it is clear that the length of ZnO nanoneedles is 10 μm with little variation. The sharp tip of the nanoneedles has the diameter of 20 nm and the length of 3 (Fig. 3C). The diameter of the trunk is 100 nm and the length is 10. Fig. 3D shows that the growth direction and lattice constant of the nanoneedles are consistent with those of bulk ZnO. Inset is the selected area of electron diffraction (SAED) pattern corresponding to (Fig. 3D). The spacing between adjacent lattice planes in the HRTEM images was found to be 0.52 nm. This is consistent with the distance between two (0001) crystal planes (c = 0.52 nm) of ZnO, confirming that the nanoneedles grow along [0001] direction (Fig. 3D). Zinc oxide nanoneedle of the sample arranged neatly which is different from the literature[14].

Growth of ZnO nanoneedles array has three stages including nucleation process, growth of the trunk and growth of the tip. The temperature of Si substrate was maintained at 700 ºC, while the temperature of ZnO powder was 1350 ºC. When ZnO powder was heated to the decomposition temperature, the vapour of Zn and O was transported to the growth zone on the Si substrate surface. The temperature of growth zone and the saturated vapour pressure (P_0) are low, the vapour supersaturation ($\Delta P/P_0$) is relatively high and the nucleation energy barrier is low. Under these conditions, ZnO nanoclusters were

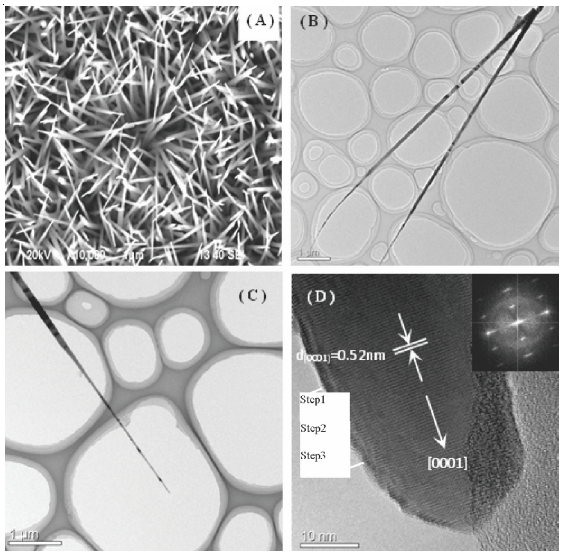

Fig. 3. (A) SEM images. (B) low magnification-TEM images of the whole ZnO nanoneedle. (C) low magnification-TEM images of the tip of ZnO nanoneedle. (D) HRTEM images of the tip of ZnO nanoneedle, inset is SAED pattern corresponding to (D)

generated on the substrate and crystallized as ZnO film (Fig. 4). The ZnO film was produced at 700 ºC for 5 min and the size of ZnO grain is 100 nm, consistent to the diameter of ZnO nanoneedles.

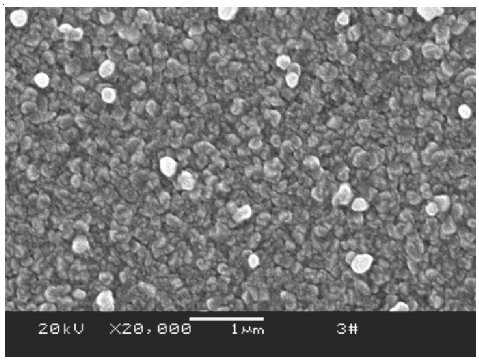

Fig. 4. SEM image of the ZnO thin film synthesized for 5 min

The ZnO grain grew along [0001] direction at 700 ºC on the substrate surface for 25 min, which became ZnO nanorods. When ZnO powder was heated to 1450 ºC, the tip of ZnO nanoneedles started to form. The process of growth is shown schematically in Fig. 5. The growth mechanism of ZnO nanoneedles array is consistent with step kinetics and bizarre surface growing and the crystal growth is a typical simple-two-dimensional-nucleation normal-layer-growth[15]. The growth surface is round bizarre surface with small size of 100 nm. Suppose that r_0 is the initial radius of two-dimensional nuclear and R is the radius of ZnO nanorods, t_s is the elapsed time of a circle step movement from r_0 to R and t_n is the elapsed time of increasing by one step along normal direction, V_s is the velocity of round step motion and V_n is the velocity of growth along normal direction. While, a new round step emerges and grows after the former one moves to edge of the nanorod along radial direction. Under this condition the nanorod grows along radial direction. While, the former round step cannot move to the edge of the nanorod along radial direction but a new one

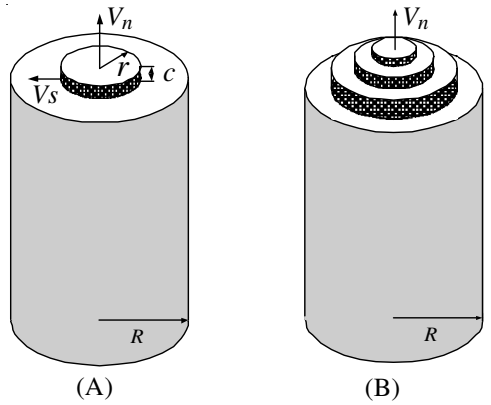

Fig. 5. Schematic of the growth of ZnO nanoneedles: (a) growth of nanorod. (b) formation of tip

emerges and grows. So the needle tip is formed on the top of the trunk, consistent with the HRTEM image (Fig. 3D) in which some steps were observed.

Fig. 6 displays the photoluminescence spectrum of ZnO nanoneedles using a Xe lamp with an excitation wavelength of 340 nm at room temperature. A sharp peak in vicinity of band edge was observed at 389 nm, which was generated because of an exciton related recombination[16]. The energy difference between 380 and 389 nm is 0.073 eV, which is the energy of a simple LO phonon. So the peak of 380 nm is a simple phonon (LO) sideband of 389 nm. On the other hand, a deep level emission, known to be related to structural defects[17], was found at 480 nm (Fig. 6).

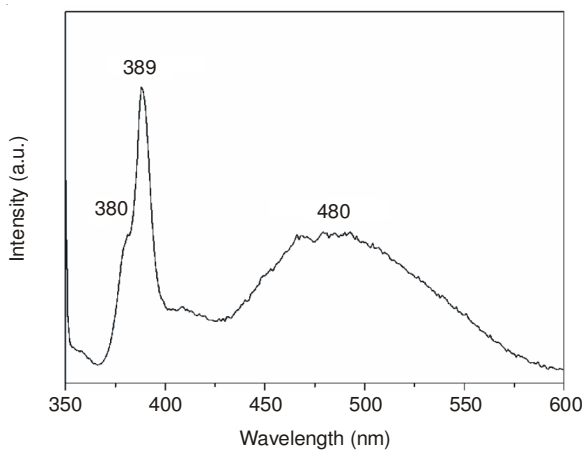

Fig. 6. Photoluminescence spectrum of ZnO nanoneedles using Xe lamp of 340 nm as incident light at room temperature

Conclusion

Zinc oxide nanoneedles array were prepared by changing the temperature of growth. The HRTEM, SEM and XRD results showed that the nanoneedles are highly crystalline in nature and grow along the [0001] direction. The growth mechanism of ZnO nanoneedles array is consistent with step kinetics and bizarre surface growing and the crystal growth is a typical simple-two-dimensional-nucleation normal-layer-growth. Room-temperature photoluminescence spectrum of ZnO nanoneedles array showed two near band-edge emission peaks at 380 nm and 389 nm and a deep level emission around 480 nm. The peak at 389 nm is generated because of an exciton related recombination, while the peak at 380 nm is simple phonon (LO) sideband of 389 nm.

ACKNOWLEDGEMENTS

This work was financially supported by the Education Bureau of Sichuan Province, China (11ZA025).

REFERENCES

1. D.C. Look, *Recent Mater. Sci. Eng. B*, **80**, 383 (2001).
2. A. Yoon, W.K. Hong and T. Lee, *J. Nanosci. Nanotechnol.*, **7**, 4101 (2007).
3. D.M. Bagnall, Y.F. Chen, Z. Zhu, T. Yao, S. Koyama, M.Y. Shen and T. Goto, *Appl. Phys. Lett.*, **70**, 2230 (1997).
4. M. Law, D. Sirbuly, J. Johnson, J. Goldberger, R. Saykally and P. Yang, *Science*, **305**, 1269 (2004).
5. C.J. Lee, T.J. Lee, S.C. Lyu, Y. Zhang, H. Ruh and H.J. Lee, *Appl. Phys. Lett.*, **81**, 3648 (2002).
6. B.R. Chalamala, R.H. Reuss, K.A. Dean, E. Sosa and D.E. Golden, *Appl. Phys.*, **91**, 6141 (2002).
7. Y. Li, G.W. Meng, L.D. Zhang and F. Phillipp, *Appl. Phys. Lett.*, **76**, 2011 (2000).
8. S. Park, Y. Mun, S. An, W. In Lee and C. Lee, *J. Lumin.*, **147**, 5 (2014).
9. J.B. Baxter and E.S. Aydil, *J. Cryst. Growth*, **274**, 407 (2005).
10. W.I. Park, D.H. Kim, S.W. Jung and G.-C. Yi, *Appl. Phys. Lett.*, **80**, 4232 (2002).
11. B. Liu and H.C. Zeng, *J. Am. Chem. Soc.*, **125**, 4430 (2003).
12. B.D. Yao, Y.F. Chan and N. Wang, *Appl. Phys. Lett.*, **81**, 757 (2002).
13. Z.W. Liu, C.W. Sun, J.F. Gu and Q.Y. Zhang, *Appl. Phys. Lett.*, **88**, 251911 (2006).
14. Q.F. Lu, H.X. Wei and Z.D. Hu, *Met. Soc. China*, **14**, 973 (2004).
15. N. Fujimura, T. Nishihara, S. Goto, J. Xu and T. Ito, *J. Cryst. Growth*, **130**, 269 (1993).
16. C. Xu, Y. Wang, H. Chen, G. Zhao and Y. Liu, *Mater. Res. Innov.*, **18**, 251 (2014).
17. L.L. Liew, H.Q. Le and G.K.L. Goh, *Mater. Res. Innov.*, **15**, 357 (2011).